Electrochimica Acta 324 (2019) 134882

Contents lists available at ScienceDirect

Electrochimica Acta

journal homepage: www.elsevier.com/locate/electacta

Investigation on electrochemical capture of CO_2 in p-Benzoquinone solutions by in situ FT-IR spectroelectrochemistry

Hui Fan, Longjiu Cheng, Baokang Jin*

Department of Chemistry, Anhui University, Hefei, 230601, China

ARTICLE INFO

Article history:
Received 17 October 2018
Received in revised form
1 March 2019
Accepted 12 September 2019
Available online 14 September 2019

Keywords:
p-Benzoquinone
Carbon dioxide
Electrochemical capture
In situ FT-IR spectroelectrochemistry
Stoichiometry study

ABSTRACT

The electrochemical capture of carbon dioxide in p-Benzoquinone (BQ) - acetonitrile and BQ - aqueous solutions have been investigated by cyclic voltammetry (CV). Two well-defined couples of anodic and cathodic peaks in CV curve of BQ in acetonitrile solvent are substituted by one redox couple peaks with $E_{1/2} = -0.30$ V once CO_2 is added. The absorption peak at 2348 cm^{-1} of in situ FT-IR spectroelectrochemistry indicates that CO_2 is involved in the electrochemical reactions. Cyclic voltabsorptometry (CVA) and derivative cyclic voltabsorptometry (DCVA) of BQ - acetonitrile with different concentration of CO_2 are investigated to demonstrate the reaction stoichiometry. The absorbance value of BQ at 2348 cm^{-1} is a constant during reduction process when CO_2 concentration is lower than 50%. However, there is a decrease at −1.3 V potential due to the CO_2 reduction when it is higher than 50%. This indicates the stoichiometry of $BQ^{\bullet-}$ to CO_2 is 1:1 during electrochemical capture of CO_2 in CH_3CN solution. Similar reaction between CO_2 and BQ is observed in aqueous solution. However, the stoichiometric number of $BQ^{\bullet-}$ to CO_2 is 1:2, forming $[BQ\text{-}2CO_2]^{\bullet-}$, which is finally reduced to $[BQ\text{-}2CO_2]^{2-}$. The mechanism proposed is consistent with theoretical calculation since the activation energy of $[BQ\text{-}CO_2]^{\bullet-}$ formation is much lower than that of $BQ^{\bullet-}$ reduction. The stable structures of CO_2 adduct of the reactions in aprotic and aqueous solvents are also proposed according to density functional theoretical (DFT) calculations.

1. Introduction

With the development of industrialization and increase of fossil fuel consumption, carbon dioxide, the largest greenhouse gas source, is becoming a serious environmental problem [1,2]. Therefore, strategies to decrease the CO_2 emission, such as CO_2 capture, storage, and reduction, have attracted worldwide attention. CO_2 capture is a process to capture and collect CO_2 from fuel gas. Generally, it can be classified into four techniques: pre-combustion, post-combustion, oxy-fuel combustion, and electrochemical capture [3]. In pre-combustion approach, fossil fuel is gasified and reacted to form H_2 and CO_2, which is further captured to avoid greenhouse gas emission. However, CO_2 concentration is usually high in pre-combustion capture, which is a barrier for its practical use [3]. Post-combustion capture is usually retrofitted to the existing power plants to capture CO_2 after fossil fuel combustion. CO_2 needs to be separated and compressed before post-combustion capture due to the lower partial pressure of CO_2. Therefore, it is an energy-intensive process due to solvent loss and regeneration, and CO_2 separation and compression [4]. Oxy-fuel combustion of fossil fuel is conducted in oxygen-rich gas. It requires large cryogenic air separation units for oxygen production, leading to the high cost of this technology [5]. Currently, CO_2 capture approaches relying on various types of chemical reactions, such as CO_2 with amines to form carbamates, CO_2 with aqueous ammonia to produce ammonium carbonate, dual alkali absorption, have been studied in detail [6–8]. However, there are lots of disadvantages presented in these traditional CO_2 capture methods limited its large scale use: (1) low CO_2 loading capacity [9]; (2) low CO_2 absorption rate [10]; (3) solvent loss and regeneration increase the cost [5]; (4) special equipment requirement and corrosion cause the high maintenance cost [8].

Compared with these traditional CO_2 chemical capture techniques, a precursor, supplying nucleophile to attack the electrophilic carbon atom of CO_2 to form adducts, can be easily regenerated during the CO_2 electrochemical capture process. Quinones and their derivatives have been studies widely because of their contribution in chemical and biology system [11–13]. Also, they are redox-active molecules with high binding affinity of CO_2 in

* Corresponding author.
E-mail address: bkjinhf@aliyun.com (B. Jin).

https://doi.org/10.1016/j.electacta.2019.134882
0013-4686/

their reduction state [14]. Quinone reduction in non-aqueous media is reported to undergo a "two-step one-electron" process [15,16]. BQ is reduced to the anion radical, $BQ^{\bullet-}$. And then, $BQ^{\bullet-}$ reacts with CO_2 immediately, leading to O—C bond or C—C bond formation. The O—C bond has better thermodynamic stability according to Gibbs free energy calculation. The electrochemical reduction of BQ in aprotic solvent has been widely studied previously. G. March et al. and B. Jin et al. proposed the two-step one-electron (EE) transfer of BQ electrochemical behavior in buffer solution, aqueous solution, and acetonitrile solvent, respectively [15,16]. BQ is reduced in normal EE mechanism, forming $BQ^{\bullet-}$ in the first step and the dianion BQ^{2-} in the second step. Actually, the research on the electrochemical capture of CO_2 by quinones has become research focus. Wrighton and Mizen proposed that after the process of electrochemical capture, two molecules of CO_2 add to reduced 9,10-phenanthrenequinone (PAQ) in $CH_3CN/[n\text{-}Bu_4N]BF_4$ to give the bis(carbonate) [17]. M. Namazian et al. studied the electrochemical reduction process of BQ in CO_2 DMF solvent [18]. M.C. Stern designed the configurations of an electrochemically-modulated process capturing and regenerating CO_2 with high efficiency using benzoquinone [19]. However, only electrochemical result is not enough to confirm the proposed mechanism of the capture of CO_2 by the electrochemical reduction product of quinone. The specific structure of the intermediate and final product produced by CO_2 capture during electrochemical reduction of benzoquinone is also uncertain. Hence, more extensive techniques should be used to investigate the mechanism of CO_2 electrochemical capture in benzoquinone. In addition, current researches are concentrated on non-aqueous systems. Compared with organic solvents, water is green, non-toxic, and cheap. Therefore, electrochemical capture of carbon dioxide in aqueous solutions should be focused on in future study.

In this paper, infrared spectroscopy combined with cyclic voltammetry is employed to investigate the electrochemical capture of CO_2 in BQ − based acetonitrile and aqueous solutions. Cyclic voltabsorptometry (CVA) is used to quantify the concentration variation of $[BQ\text{-}CO_2]^{2-}$ and CO_2. The stoichiometry of electrochemical capture of CO_2 is proposed with different concentrations of CO_2 both in acetonitrile and aqueous solutions by CV and CVA. The results show that the mechanisms of BQ in acetonitrile in the presence of CO_2 are different from that in aqueous solution. The possible structures of anion radical and dianion (CO_2 adducts) are explored by density functional theoretical calculation.

2. Experimental section

2.1. Chemicals and reagents

BQ (97%), acetonitrile (HPLC), D_2O (HPLC), tetrabutylammonium perchlorate (TBAP) and KCl are all used as received from Sigma-Aldrich. 0.2 mmol/L TBAP and 0.5 mol/L KCl are used as supporting electrolyte in acetonitrile and H_2O, respectively. High purity carbon dioxide (Nanjing special gas Co. Ltd, CO2 (99.99%), and high purity Ar (Nanjing special gas Co. Ltd, (99.99%) are used for Solution A (with saturated CO2) and Solution B (BQ degassed with Ar), respectively. Solution A and solution B are mixed with different volume fractions, and then BQ solutions with different CO_2 concentrations are prepared.

2.2. Electrochemistry

Electrochemical experiments are performed with an electrochemical analyzer CHI630 potentiostat (Shanghai Chenhua Instruments). The homemade thin-layer is used as a spectroelectrochemical cell [20]. A 4 mm diameter platinum disk electrode is used as a working electrode [21]. It is polished with alumina slurry on a polishing cloth initially, and then rinsed in deionized water and ethanol before use. Ag/AgCl and a platinum wire electrode are employed as reference electrode and counter electrode, respectively [14,22].

2.3. In situ FT-IR spectroelectrochemistry

In situ FT-IR spectroelectrochemistry experiments and electrochemical measurements are carried out simultaneously. Nicolet iS50 (Thermo Nicolet Corporation) spectrometer equipped with a specular reflectance accessory (SMART iTR) and a HgCdTe/A (MCT/A) detector cooled with liquid nitrogen are employed in spectroscopic measurement. A total of 20—60 interferometric scans are accumulated for an averaged spectrum in subtractively normalized interfacial fourier transform infrared (SNIFTIR) experiment with a resolution of 16 cm^{-1}, and the sampling interval is 0.7—1.8 s. Experimental results are depicted with Grams/3D software.

2.4. Theoretical computation

All theoretical calculations are implemented in Gaussian 09 package. Structural optimizations and frequency calculations (corresponding characteristic infrared spectrum wave numbers) are carried out using the hybrid B3LYP method with the basis set of 6-311 + G** level of theory with the solution effect [23,24].

3. Results and discussions

3.1. Electrochemical capture of CO_2 in BQ - acetonitrile solution

Fig. 1A shows the cyclic voltammograms curve of acetonitrile containing single CO_2 (curve a), BQ without (curve b) and with CO_2 (curve c). As shown in Fig. 1A (a), there is no Faraday current observed in CV curve in scan range of +0.2 V to −1.2 V. In Fig. 1A (b), a typical CV curve of BQ in aprotic media is observed with two well-defined couples of anodic and cathodic peaks, with potential values of $^1E_{1/2} = -0.39$ V and $^2E_{1/2} = -0.73$ V (defined $E_{1/2} = (E_{pa}+E_{pc})/2$). This is in accordance with previous reports [16]. However, there is only one redox couple with $E_{1/2} = -0.30$ V observed when CO_2 is added (voltammogram c). Moreover, the cathodic peak current is almost double as that of voltammogram (b). Obviously, the CV of BQ with CO_2 is similar to that of BQ in acetonitrile solvent with added proton donors [25]. Therefore, the second couple of redox peak shifts positively and merges with the first one, which might be related to chemical reaction of CO_2.

The rapid-scan IR spectra is simultaneously conducted and recorded from 1000 cm^{-1} to 3000 cm^{-1} during the electrochemical process (Fig. 1B). The 3D rapid-scan IR spectra are gathered during the CV scan between 0.2 V and −1.2 V with reference spectrum recorded at 0.2 V. There are two types of IR bands observed in the 3D spectra. One type is downward band at 2348 cm^{-1} (assigned to $\nu_{C=O}$ of CO_2), and the other type is the upward bands at 1249 cm^{-1}, 1356 cm^{-1}, 1518 cm^{-1}(assigned to $\nu_{C=C}$ and $\nu_{C\text{-}O}$ of the finial product dianion $(BQ\text{-}CO_2)^{2-}$), and 1641 cm^{-1} (assigned to $\nu_{C=O}$ of reduction product of $(BQ\text{-}CO_2)^{2-}$). The characteristic absorption peak at 2348 cm^{-1} suggests that CO_2 is involved in the electrochemical reaction. This implies the chemical reaction between CO_2 and $BQ^{\bullet-}$ because CO_2 cannot be electrochemical reduced in this potential range [26].

To illustrate CO_2 absorption behavior, the rapid-scan IR spectra is conducted to CVA to track the concentration variation of $(BQ\text{-}CO_2)^{2-}$ and CO_2 (Fig. 2A). According to Fig. 2A, there is a significant increase of absorbance at 1356 cm^{-1}, while a dramatical decrease of absorbance is observed at 2348 cm^{-1}. The absorbance variation at

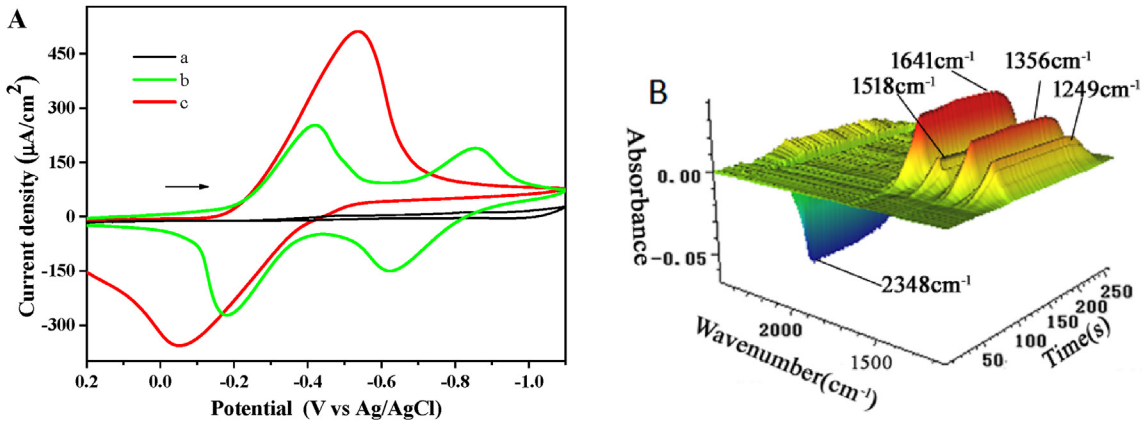

Fig. 1. (A) CV of: (a) only saturated CO_2, (b) only 20 mmol/L BQ, (c) 20 mmol/L BQ with saturated CO_2 in acetonitrile containing 0.2 mmol/L TBAP, (B) 3D in-situ FT-IR spectra of solution. The scan rate was 10 mV/s.

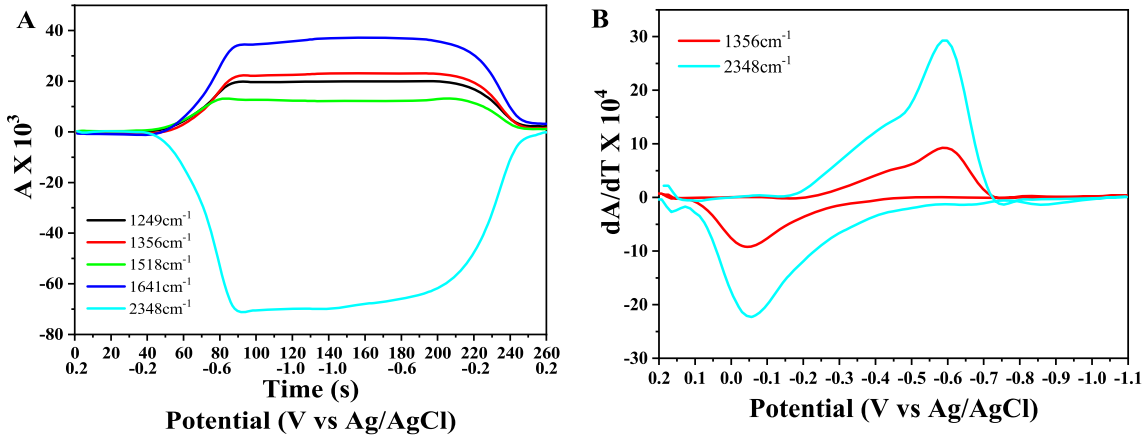

Fig. 2. CVA and DCVA of BQ at 1249 cm^{-1}, 1356 cm^{-1}, 1518 cm^{-1}, 1641 cm^{-1}, 2348 cm^{-1}. To make the DCVA data readily comparable to CV, the DCVA of 2348 cm^{-1} was multiplied by −1.

1641 cm^{-1} $(BQ\text{-}CO_2)^{2-}$ is similar to that at 1356 cm^{-1}. As the potential (time) scanning, the original electrochemical reduction intermediates, $BQ^{\bullet-}$ [25], combines with CO_2 immediately after its appearance, corresponding to the reduction process maybe from BQ to $(BQ\text{-}CO_2)^{\bullet-}$, and then, $(BQ\text{-}CO_2)^{\bullet-}$ is further reduced to $(BQ\text{-}CO_2)^{2-}$ quickly.

It has been demonstrated that dA/dt vs E shape is morphologically consistent with the cyclic voltammogram [16]. According to Fig. 2B, the wave form of DCVA at 2348 cm^{-1} represents of CO_2, and 1356 cm^{-1} represents of $(BQ\text{-}CO_2)^{2-}$, which are similar to that of the CV shown in Fig. 1. A.

Different from the normal two-step one-electron transfer [16], the results of CV and IR spectroelectrochemistry with a couple of single peaks show that BQ in the presence of CO_2 undergoes a ECE transfer mechanism.

3.2. Stoichiometry study of electrochemical capture of CO_2 in BQ-acetonitrile solution

To investigate the correlation between CO_2 and BQ in the electrochemical process, CVs of 20 mmol/L BQ with different CO_2 concentration and single saturated CO_2 (marked as blank) in acetonitrile are conducted and presented in Fig. 3A. As shown in blank, there is no redox peaks appeared in the scan region of 0.2 to −1.2 V. However, a miniature irreversible reduction peak exists at about −1.6 V corresponding to 100% CO_2, indicating the electrochemical reaction of CO_2 itself [26]. There are two couples of redox peaks presented in CV curve when CO_2 concentration is 25%, and there redox potential $^1E_{1/2} = -0.42$ V and $^2E_{1/2} = -0.97$ V corresponds to the reduction of BQ [25]. The result indicates that CO_2 is consumed completely, while excessive BQ still follows EE mechanism. It is found that the reduction peak currents increase with the increase of CO_2 concentration at −0.42 V, while it decreases with the increase of CO_2 concentration at −0.97 V. In saturated CO_2 (100%) solutions, the reduction peak at 1.6 V is clearly observed, which attributes to electrochemical reduction of CO_2 itself. The corresponding 3D spectra of BQ in acetonitrile with different percentage of CO_2 concentration is provided in the supporting information.

Fig. 3B shows the corresponding CVA of BQ with different percentages of CO_2 at 2348 cm^{-1}. As can be seen from Fig. 3B, the absorbance value of BQ solution with low concentration of CO_2 (20% ~50%) at 2348 cm^{-1} decreases at about 42s (−0.21 V), and a minimum value is obtained at about 80s (−0.60 V). And the absorbance value is a constant during reduction process, which illustrates that all CO_2 is reacted with BQ. The variation of absorbance value of BQ solution with high concentration of CO_2 (75%, 100%) at 2348 cm^{-1} is the same with that of BQ solution with low concentration of CO_2 (20%~50%) initially. However, there is a further decrease at −1.3 V potential due to the reduction of CO_2, which suggested that CO_2 are

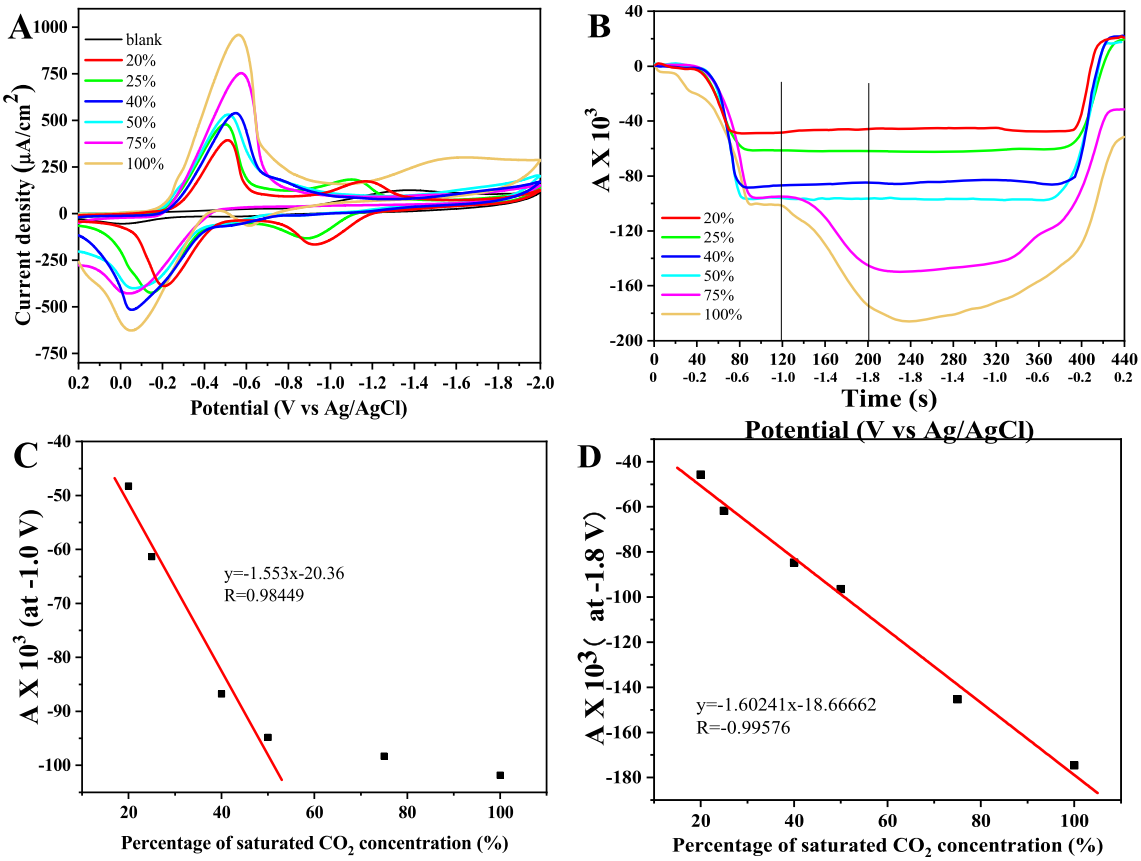

Fig. 3. (A) CV of 20 mmol/L BQ solution dissolved in acetonitrile with different percentages of CO_2, and 0.2 mmol/L TBAP is used as supporting electrolyte. The scan rate is 10 mV/s; (B) The corresponding CVA of BQ with different percentages of CO_2 at 2348 cm^{-1}; (C) Linear fitting curve of absorbance value at 2348 cm^{-1} with different percentages of CO_2 (−1.0 V); and (D) Linear fitting curve of absorbance value at 2348 cm^{-1} with different percentages of CO_2 (−1.8 V).

over capacity in high concentration of CO_2 (75%, 100%) solution. IR absorbance at 2348 cm^{-1} does not return to its initial value when the potential scan back to the original value (0.2 V), implying that the reduction product of excessive CO_2 is not completely oxidized under this potential range.

According to Lambert-Beer's law, the absorbance value at 2348 cm^{-1} reflects the change of CO_2 concentration in electrochemical process. Therefore, the absorbance value at −1.8 V is linearly related to the percentage of saturated CO_2 concentration with coefficient of determination R = 0.9958 (Fig. 3D). The fitting results further prove that CO_2 is consumed completely at −1.8 V. A similar linear relationship between CO_2 concentration and absorbance value at −1.0 V is also observed in Fig. 3C. It can be founded that the absorbance gradually decreases with the increase of CO_2 concentration at low concentration (<50%). However, the absorbance value remains unchanged when the CO_2 concentration increases further (>50%). Further analysis of the obtained linear regression equations shows that the slope of the regression curve under the low concentration CO_2 in Fig. C is consistent with that of Fig. D. The results strongly suggest that all CO_2 in the solution reacts completely with benzoquinone at −1.0 V if CO_2 concentration is less than 50%. When the CO_2 concentration is greater than 50%, excessive CO_2 can be reduced at a more negative potential (−1.3 V). The saturated CO_2 in acetonitrile media is 40 mmol/L [33]. Hence, 50% CO_2 saturated concentration is 20 mmol/L, which is equivalent to the concentration of BQ in solution. Therefore, the electrochemical process can be described as following:

3.3. Electrochemical capture of CO_2 in aqueous solution

The CV of BQ in aqueous solution with different CO_2 concentrations is studied and presented in Fig. 4. Since proton electrolyzed at the large negative potential, the scan range is limited to a small range from 0.5 V to −0.3 V to avoid its reaction potential. As shown

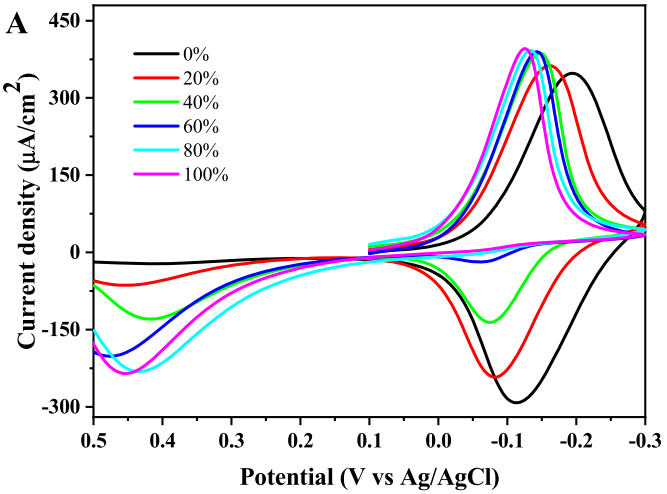

Fig. 4. CV for BQ of different percentage of saturated CO_2 concentration in aqueous solution containing 8 mmol/L BQ and 0.5 mol/L KCl as the supporting electrolyte, the scan rate was 5 mV/s.

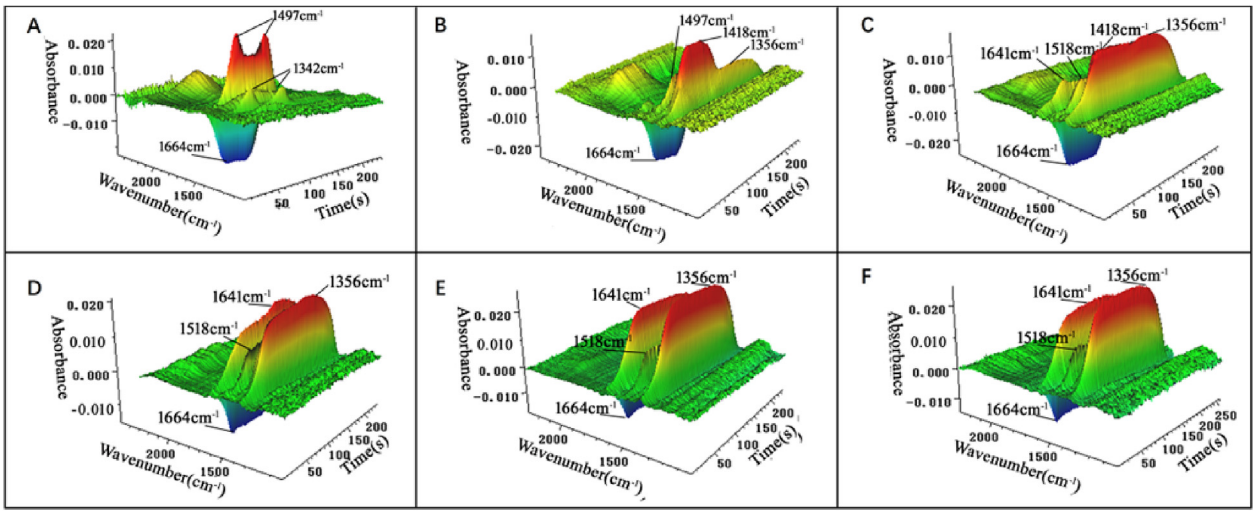

Fig. 5. 3D-in situ FT-IR spectroelectrochemistry spectra responding to the thin-layer CV of Fig. 4 of 8 mmol/L BQ in D_2O with varying CO_2 concentration (A:0%, B:20%, C:40%, D:60%, E:80%, F:100%).

in Fig. 4, a couple of redox peaks are observed with potential values of $^1E_{1/2} = -0.17$ V (defined $E_{1/2} = (E_{pa}+E_{pc})/2$) in the absence of CO_2 [16]. The reduction peak of BQ moves positively with the gradual increase of CO_2 concentration, and the reduction peak area is almost a constant.

However, the oxidation peak shifts positively with peak current gradually decreased from −36.49 μA to −0.49 μA when CO_2 concentration increases from 0% to 80%. Meanwhile, a new oxidation peak appears at about +0.43 V with the increase of CO_2 concentration, and the maximum peak current of −29.18 μA is obtained at 80% of CO_2.

The rapid - scan IR spectroelectrochemistry analysis of quinone aqueous solution with different CO_2 concentration is conducted to explore the mechanism of CO_2 captured during the reduction of quinone in aqueous solution. D_2O is used to replace H_2O to avoid the interference (H_2O generates serious infrared noise). As presented in Fig. 5, infrared absorption peaks of intermediates in aqueous solution without CO_2 (1497 cm^{-1}, assigned to $\nu_{C=O}$ of $BQ^{\bullet-}$ in aqueous) periodically appear and disappear in both reduction and oxidation process, which are similar to that of benzoquinone in acetonitrile solution. Although only one pair of redox peaks appears in the CV diagram (Figs. 4 and 0%), the intermediate absorption peaks in the infrared spectra indicates that benzoquinone exhibits a "two-step one-electron transfer" in aqueous solution [16].

IR peaks at 1664 cm^{-1}, 1356 cm^{-1} and 1641 cm^{-1} are selected to track the electrochemical process of 8 mmol/L BQ in D_2O solution with CO_2 (Fig. 5B–F). The CO_2 absorbance peaks at 1497 cm^{-1} (assigned to $\nu_{C=O}$ from $BQ^{\bullet-}$) and 1342 cm^{-1} (assigned to $\nu_{C=C}$ from $BQ^{\bullet-}$) reduce dramatically, and finally disappears when CO_2 concentration is 40% (Fig. 5C). The absorbance peak at 1418 cm^{-1} (assigned to $\nu_{C=C}$ from BQ^{2-}) gradually decreases with the increase of CO_2 concentration, and cannot be observed in 60% CO_2 (Fig. 5D). There are no peaks in the 3D IR spectrum observed at 1497 cm^{-1}, 1342 cm^{-1}, 1418 cm^{-1} when CO_2 concentration is higher than 60%. Meanwhile, there are new absorption peaks observed at 1518 cm^{-1}, 1641 cm^{-1} and 1356 cm^{-1}, assigned to ν_{C-C}, $\nu_{C-C=O}$ and $\nu_{C=C}$ from $(BQ\text{-}CO_2)^{2-}$. The results indicate that the intermediate $BQ^{\bullet-}$ rapidly reacts with CO_2 to form $(BQ\text{-}CO_2)^{\bullet-}$, and then, it accepts the second electron quickly to form dianion $(BQ\text{-}CO_2)^{2-}$ in the presence of CO_2. Eventually, four peaks of IR peaks are observed under the condition of high concentration of CO_2 (>60%), the

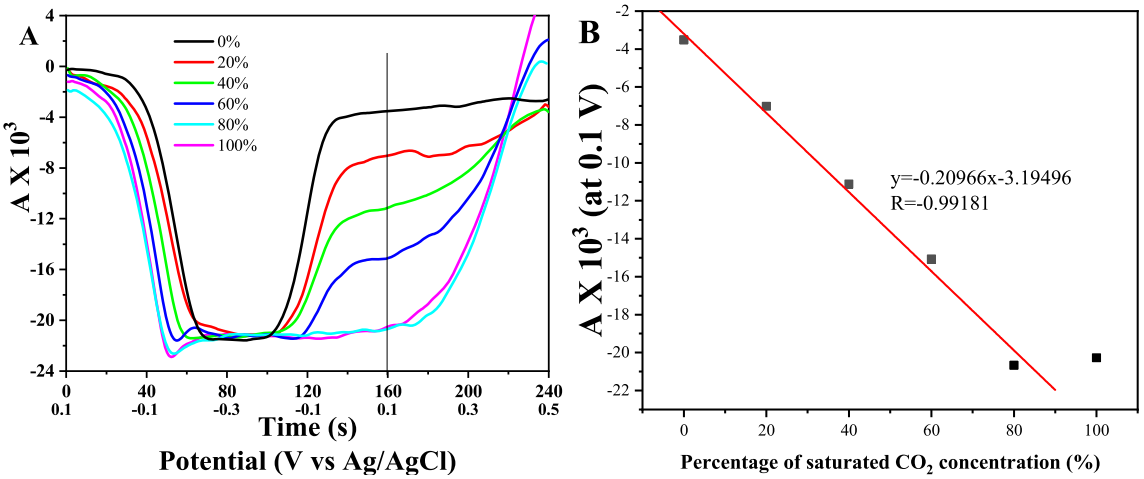

Fig. 6. (A) The CVA at1664 cm^{-1} in different concentrations of CO_2; (B) the linear fitting curve of absorbance value at 1664 cm^{-1} with percentage of saturated CO_2 concentration (0.1 V).

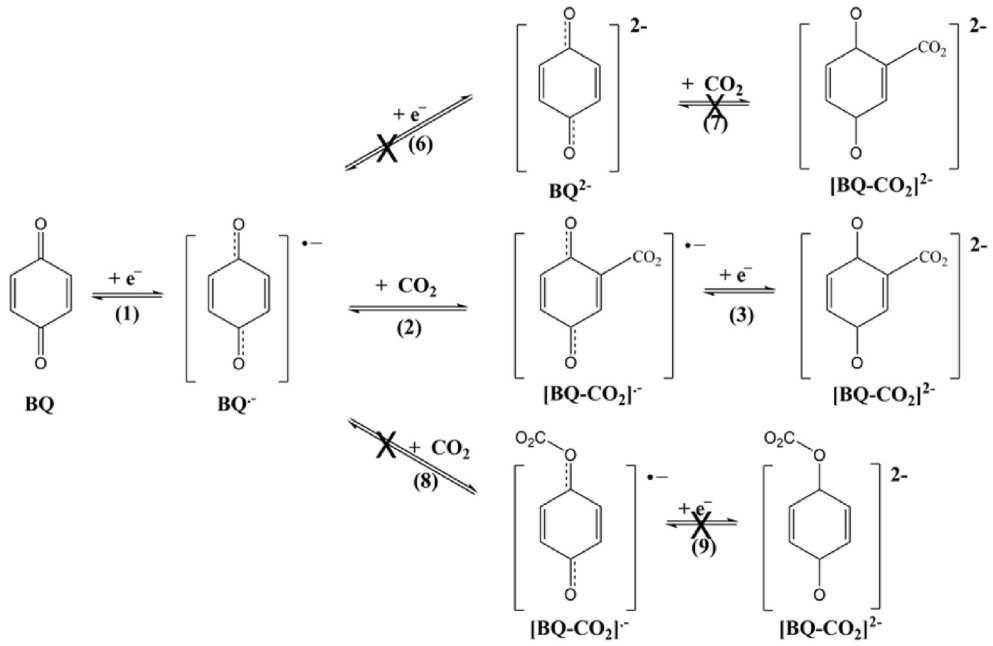

$$BQ \overset{e^-}{\rightleftharpoons} BQ^{\bullet -} \quad (1)\ E^0_1$$

$$BQ^{\bullet -} + CO_2 \rightleftharpoons [BQ\text{-}CO_2]^{\bullet -} \quad (2)\ E^0_2$$

$$[BQ\text{-}CO_2]^{\bullet -} \overset{e^-}{\rightleftharpoons} [BQ\text{-}CO_2]^{2-} \quad (3)\ E^0_3$$

$$BQ^{\bullet -} \overset{e^-}{\rightleftharpoons} BQ^{2-} \quad (6)\ E^0_6$$

$$BQ^{2-} + CO_2 \rightleftharpoons [BQ\text{-}CO_2]^{2-} \quad (7)\ E^0_7$$

Scheme 1. Reaction process of BQ in the presence of CO_2 in aprotic solvent (reduction 1, 3, and 4), E^0: activation energy of the reaction.

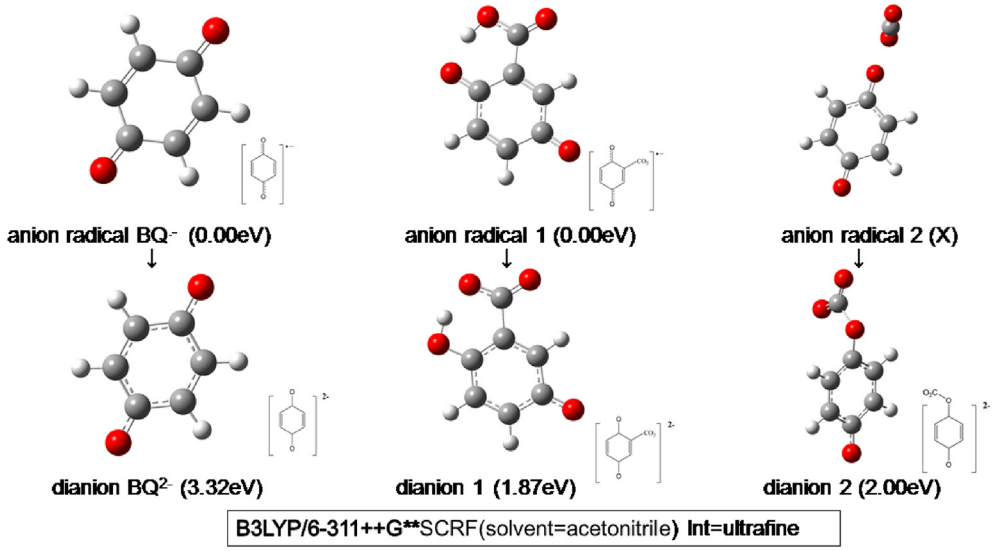

Fig. 7. The monomer and low-energy isomers for anion radical and dianion in acetonitrile solvent at B3LYP/6-311++G** level and corresponding possible structures of anion radical and dianion. X indicates instability.

Table 1
The assignment of infrared absorption peak in acetonitrile solvent.

Experimental Peak position(cm^{-1})	Assignation	Calculated Peak position(cm^{-1})		Solvent
		Dianion 1	Dianion 2	
1249	Bending vibration $\nu_{C\text{-}C=O}$ from $[BQ\text{-}CO_2]^{2-}$	1258	1242	aprotic solution
1356	Stretching vibration $\nu_{C=C}$ from $[BQ\text{-}CO_2]^{2-}$	1371	1383	aprotic solution
1518	Bending vibration $\nu_{C\text{-}C=O}$ from $[BQ\text{-}CO_2]^{2-}$	1540	1581	aprotic solution
1641	Stretching vibration $\nu_{C\text{-}C=O}$ from $[BQ\text{-}CO_2]^{2-}$	1620	1695	aprotic solution
1664	Stretching vibration $\nu_{C=O}$ from BQ	1676		aprotic solution
2348	Stretching vibration $\nu_{C=O}$ from CO_2	2346		aprotic solution

upward peaks 1518 cm^{-1}, 1641 cm^{-1}, 1356 cm^{-1} and downward peak 1664 cm^{-1}. The absorbance of 1356 cm^{-1} increases simultaneously with the decrease of 1664 cm^{-1} in the reduction process, and recovers to the original value while $(BQ\text{-}CO_2)^{2-}$ is oxidized at the end of potential scans. These changes of absorption peaks clearly illustrate the dominant reaction mechanism in the system changes from EE mechanism to EC_rE mechanism in the presence of CO_2.

The corresponding CVA of BQ at 1664 cm^{-1} in different concentrations of CO_2 is depicted in Fig. 6A. As it shows, the peak value starts to decrease at 28s (−0.04 V), and a minimum value is observed at 72s (−0.26 V). Similarly, it increases from 93s (−0.24 V) to 124s (−0.08 V) and restores to the original value in the oxidation process, which indicates that BQ is reduced to BQ^{2-} completely at −0.26 V, and then all reduction product is oxidized back to BQ. This result is consistent with the CV results (Fig. 4), which might be due to the easier reduction of BQ caused by the combination of CO_2 with reduction states of BQ. Interestingly, during the oxidation process, the infrared absorption peaks at 1664 cm^{-1} show a tendency to change in relation to CO_2 concentration. The absorbance value gradually change in solution with 20%–60% CO_2 concentration until became stable in 80% and 100% solution.

The infrared absorption peak of BQ aqueous solution containing 40% CO_2 begins to rise at 103s (−0.19 V), and reach a stable value at 148s (0.04 V) when BQ^{2-} is oxidized to BQ. While the potential scanning positive, it will rise again at 180s (0.20 V) and finally comes back to baseline. The second rise of the infrared absorption peaks at 1664 cm^{-1} corresponds to second oxidation peaks in the CV diagram. A reasonable explanation is that BQ is excessive in low concentration CO_2 solution. Therefore, excess BQ^{2-} existing in the reduction process is oxidized at −0.1 V, whereas BQ^{2-} bound to CO_2 is oxidized at 0.2 V.

It can be observed clearly from Fig. 6A that the amplitude of the first increase (100s–140s) of infrared absorption peak at 1664 cm^{-1} decreases with the increase of CO_2 concentration. In the BQ aqueous solution with saturated CO_2 (100%), the step of the first rise of the infrared absorption peak completely disappeared. Similar results were observed in BQ solution with a concentration of 80% CO_2. From the results of CV (Fig. 4) and CVA (Fig. 6A), it can be found that BQ^{2-} has been completely oxidized to BQ, but $(BQ\text{-}CO_2)^{2-}$ still exists stably in the oxidation process when the potential is lower than 0.1 V. Therefore, the infrared absorbance value at 0.1 V can reflect the amount of $(BQ\text{-}CO_2)^{2-}$ in solution.

Fig. 6B reveals the relationship between the CO_2 concentration

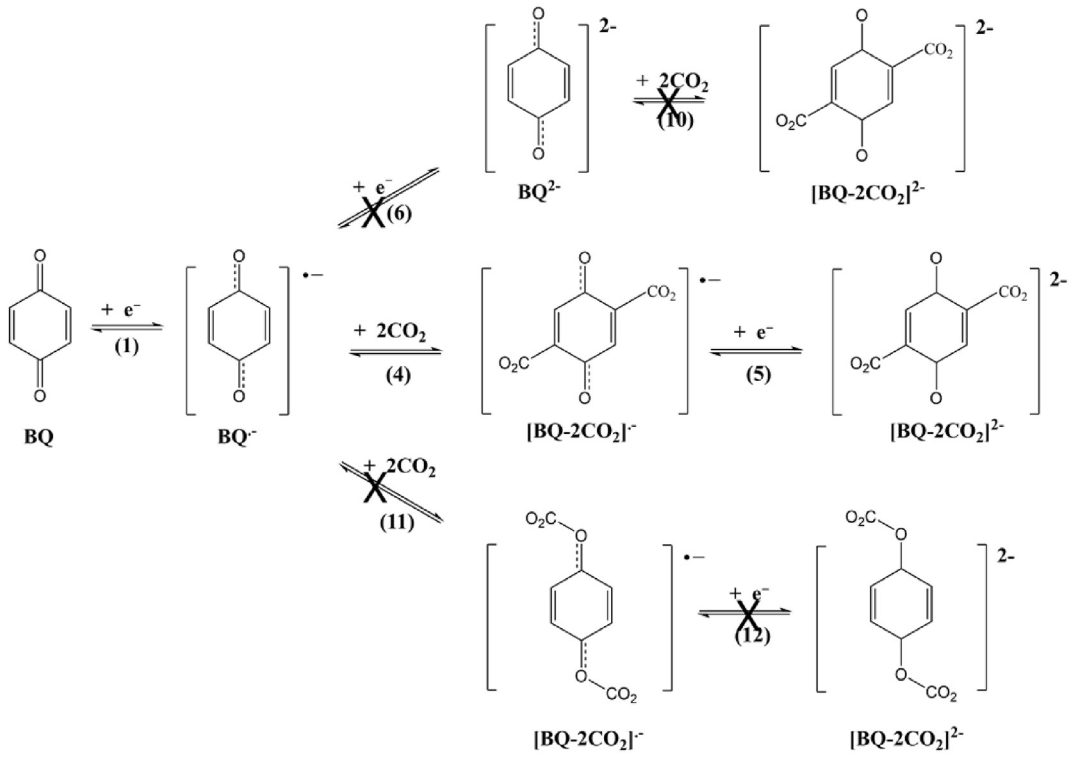

Scheme 2. Reaction process of BQ in the presence of CO_2 in H_2O solvent (reaction 1, 4and 5).

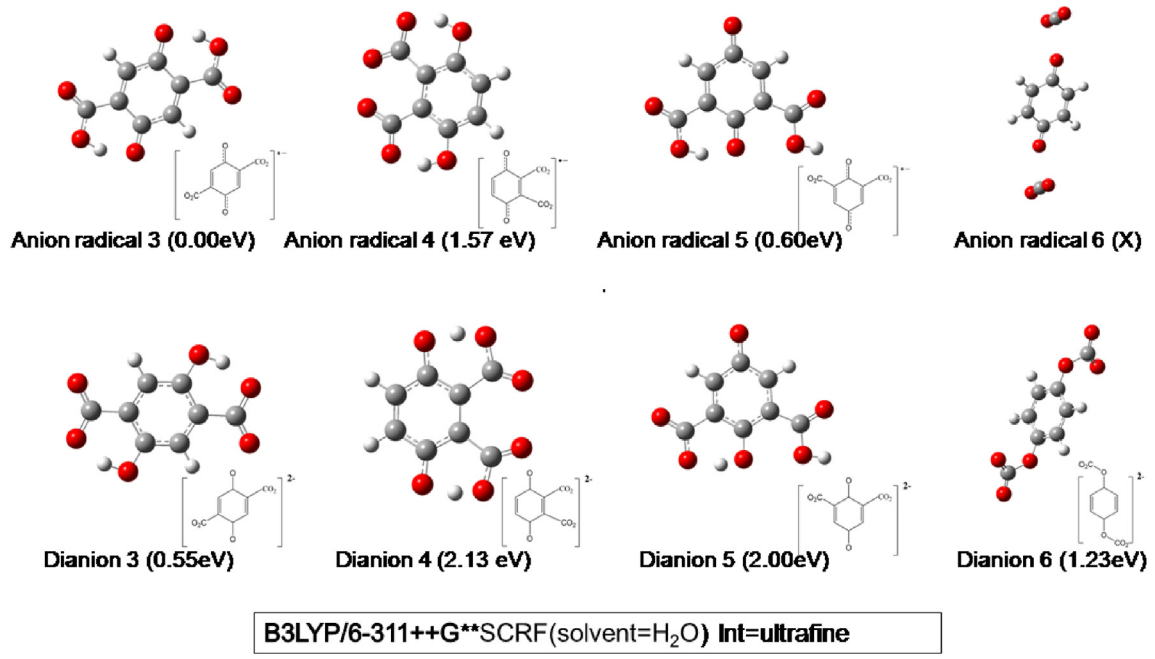

Fig. 8. The monomer and low-energy isomers for anion radical and dianion in H_2O solvent at B3LYP/6-311++G** level and corresponding possible structures of anion radical and dianion.

and IR absorbance value (2348 cm^{-1}) at 0.1 V. As expected, the concentration of CO_2 in 0%–80% is linearly related to the infrared absorption value, implying that 80% CO_2 can react completely with BQ. However, CO_2 is obviously excessive in saturated CO_2 (100%) solutions because the IR absorbance value is not lineally related to CO_2 concentration. The concentration of CO_2 saturated aqueous solution is 20 mmol/L [27]. 80% saturated CO_2 concentration is 16 mmol/L, which is double to the concentration of BQ (8 mmol/L) in solution. Therefore, the electrochemical process can be described as follows:

3.4. Theoretical computation

Based on the experimental data analysis above, several possible electrochemical reaction mechanisms of BQ in the presence of CO_2 in aprotic solvent are theorized in the Scheme 1. The activation energies of reactions are computed by theoretical computation.

As shown in Scheme 1, BQ in aprotic solvent gets an electron to form $BQ^{\bullet-}$ in reaction (1) firstly. $BQ^{\bullet-}$ captures CO_2 immediately (the activation energy E^0_2 is 0.45eV), rather than reduces to BQ^{2-} (E^0_6 is 3.32eV) ($E^0_2<E^0_6$), which is consistent with the only one pair peaks observed in CV diagram. Then, $[BQ\text{-}CO_2]^{\bullet-}$ is reduced to form $[BQ\text{-}CO_2]^{2-}$ (E^0_3 is 1.87eV). Combining with the results of electrochemical and infrared spectroscopy, we speculate that the reduction of BQ in the presence of CO_2 undergoes the reaction (1), reaction (2), and reaction (3) in sequence. BQ is reduced to $BQ^{\bullet-}$ in the first step, then $[BQ\text{-}CO_2]^{\bullet-}$ is generated through the chemical reaction of $BQ^{\bullet-}$ with CO_2. Furthermore, the anion radical ($[BQ\text{-}CO_2]^{\bullet-}$) quickly reduces to dianion ($[BQ\text{-}CO_2]^{2-}$) in the second electrochemical step.

The possible structures and relative energy of the anion radical and dianion are considered and listed in Fig. 7. For anion radical ($[BQ\text{-}CO_2]^{\bullet-}$), two kinds of anion radical have been calculated. The results of theoretical computation show carboxylate product (anion radical 1) is more thermodynamic stable than the carbonate one (anion radical 2). The anion radical 2 is not able to be further reduced to form dianion. Based on the density functional theory, dianion 1 is easy to form since dianion 1 is much lower in energy (1.87eV) than that of dianion 2 (2.00eV). The calculation shows that the anion radical and dianion exist in the form of carboxylate product.

The theoretical value of infrared absorption peak position is given in Table 1. The characteristic infrared absorption peak positions of carboxylate structure dianion 1 and carbonate structure

Table 2
The assignment of infrared absorption peak in H_2O solvent.

Experimental Peak position(cm^{-1})	Assignation	Calculated Peak position(cm^{-1})		Solvent
		Dianion 3	Dianion 6	
1279	Bending vibration $\nu_{C\text{-}C=O}$ from $[BQ\text{-}2CO_2]^{2-}$	1283	1149	H_2O solution
1342	Stretching vibration $\nu_{C=C}$ from $BQ^{\bullet-}$	1356		H_2O solution
1356	Stretching vibration $\nu_{C=C}$ from $[BQ\text{-}2CO_2]^{2-}$	1369	1273	H_2O solution
1418	Stretching vibration $\nu_{C=O}$ from $[BQ]^{2-}$	1431		H_2O solution
1497	Stretching vibration $\nu_{C=O}$ from $[BQ]^{\bullet-}$	1489		H_2O solution
1518	Stretching vibration $\nu_{C\text{-}C}$ from $[BQ\text{-}2CO_2]^{2-}$	1528	1487	H_2O solution
1641	Stretching vibration $\nu_{C\text{-}C=O}$from$[BQ\text{-}2CO_2]^{2-}$	1624	1748	H_2O solution
1664	Stretching vibration $\nu_{C=O}$ from BQ	1676		H_2O solution
2348	Stretching vibration $\nu_{C=O}$ from CO_2	2346		H_2O solution

dianion 2 are calculated respectively, which are multiplied by the frequency correction factor of the algorithm B3TYP/6-311 + G**, 0.976 [23]. The corresponding results are compared with the experimental infrared peak position. As shown in Table 1, the result of carboxylate product is closer to that of experimental data, which further proofs the rationality of mechanism.

Similarly, BQ undergoes the electron transfer, chemical reaction and further electron transfer process with CO_2 in aqueous solution. However, it should be noted that 1 mol $BQ^{\bullet-}$ combines with 2 mol CO_2 in the chemical reaction process. The whole reaction is chemical reversible (Scheme 2).

The possible structures and relative energy of anion radical and dianion of the reaction in aqueous solvent are also calculated. Since the stoichiometric ratio of BQ to CO_2 is 1:2, four kinds of anion radical ($[BQ\text{-}2CO_2]^{\bullet-}$) are calculated as listed in Fig. 8 (the energy of anion radical 3 is defined as 0.00eV). As shown in theoretical computation results, anion radical 4 and 5 have higher energy value with virtual frequency, the calculation result of anion radical 6 is unable to converge. In contrast, anion radical 3 is the structure with the lowest energy value and could further reduce to dianion 3 ($[BQ\text{-}2CO_2]^{2-}$) in the second electrochemical step. Thus, the anion radical 3 is the most stable anion radical structure.

As shown in Table 2, the experimental and theoretical value of IR absorbance peak position is also listed. And the frequency correction factor is 0.976 [24]. The theoretical value of characteristic absorption peak position of carboxylate structure is closer to the experimental data, which is consistent with the previous inference.

4. Conclusions

In this paper, the electrochemical redox mechanisms of BQ in the presence of CO_2 in aprotic media, and aqueous solvent are explored through CV and in situ FT-IR spectroelectrochemistry. Three conclusions are obtained according to our study:

1. The results of CV and FT-IR spectroelectrochemical analysis indicated that the presence of CO_2 leading to a chemical reaction between $BQ^{\bullet-}$ and CO_2. Then $[BQ\text{-}CO_2]^{\bullet-}$ is further reduced to $[BQ\text{-}CO_2]^{2-}$.
2. Further CVA and density functional theoretical calculation were conducted for quantitative analysis. The stoichiometric number of $BQ^{\bullet-}$ to CO_2 is 1:1 in acetonitrile, while which is 1:2 in aqueous solvent, thus:

in CH_3CN solvent,

$$BQ \overset{e^-}{\rightleftharpoons} BQ^{\bullet-}$$
$$BQ^{\bullet-} + CO_2 \rightleftharpoons [BQ\text{-}CO_2]^{\bullet-}$$
$$[BQ\text{-}CO_2]^{\bullet-} \overset{e^-}{\rightleftharpoons} [BQ\text{-}CO_2]^{2-}$$

in aqueous solvent,

$$BQ \overset{e^-}{\rightleftharpoons} BQ^{\bullet-}$$
$$BQ^{\bullet-} + 2CO_2 \rightleftharpoons [BQ\text{-}2CO_2]^{\bullet-}$$
$$[BQ\text{-}2CO_2]^{\bullet-} \overset{e^-}{\rightleftharpoons} [BQ\text{-}2CO_2]^{2-}$$

3. The possible structures and energy of anion radical and dianion are calculated at B3LYP/6-311++G** level, indicating the carboxylate is the stable product for $BQ^{\bullet-}$ react with CO_2. Furthermore, the theoretical calculation value of the infrared characteristic absorption peak is identified the final product corresponding to the experimental infrared peak position, which proves the proposed electrochemical mechanism.

Acknowledgment

This work has been supported by the National Nature Foundation of China (Grant 21375001 and 21273008), Doctoral Program Foundation of the Ministry of Education of China (201034011110001), and the Foundation of Scientific Innovation Team of Anhui Province (2006KJ007TD), China.

Appendix A. Supplementary data

Supplementary data to this article can be found online at https://doi.org/10.1016/j.electacta.2019.134882.

References

[1] H. Wei, J. Chen, N. Fu, H. Chen, H. Lin, S. Han, Electrochim. Acta 266 (2018) 161–169.
[2] R. De Motte, R. Mingant, J. Kittel, F. Ropital, P. Combrade, S. Necib, V. Deydier, D. Crusset, Electrochim. Acta 290 (2018) 605–615.
[3] S.D. Kenarsari, D. Yang, G. Jiang, S. Zhang, J. Wang, A.G. Russell, Q. Wei, M. Fan, RSC Adv. 3 (2013).
[4] P. Yuan, Z. Qiu, J. Liu, IOP Conf. Ser. Earth Environ. Sci. 64 (2017).
[5] B.P. Spigarelli, S.K. Kawatra, J. CO2 Util. 1 (2013) 69–87.
[6] P. Singh, J.H. Rheinhardt, J.Z. Olson, P. Tarakeshwar, V. Mujica, D.A. Buttry, J. Am. Chem. Soc. 139 (2017) 1033–1036.
[7] K.P. Resnik, H.W. Pennline, Fuel 105 (2013) 184–191.
[8] A.A. Olajire, Energy 35 (2010) 2610–2628.
[9] H. Herzog, D. Golomb, Encyclopedia Energy 1 (2004) 1–11.
[10] J.T. Cullinane, G.T. Rochelle, Chem. Eng. Sci. 59 (2004) 3619–3630.
[11] T.M. Alligrant, J.C. Hackett, J.C. Alvarez, Electrochim. Acta 55 (2010) 6507–6516.
[12] P.D. Astudillo, D.P. Valencia, M.A. González-Fuentes, B.R. Díaz-Sánchez, C. Frontana, F.J. González, Electrochim. Acta 81 (2012) 197–204.
[13] P.N. Refojo, M. Teixeira, M.M. Pereira, BBA - Bioenergetics 1817 (2012) 1852–1859.
[14] B. Gurkan, F. Simeon, T.A. Hatton, Acs Sustainable Chemistry 3 (2015) 1394–1405.
[15] G. March, S. Reisberg, B. Piro, M.C. Pham, M. Delamar, V. Noel, K. Odenthal, D.B. Hibbert, J.J. Gooding, J. Electroanal. Chem. 622 (2008) 37–43.
[16] B. Jin, J. Huang, A. Zhao, S. Zhang, Y. Tian, J. Yang, J. Electroanal. Chem. 650 (2010) 116–126.
[17] M.B. Mizen, M.S. Wrighton, J. Electrochem. Soc. 136 (1989) 941–946.
[18] M. Namazian, H.R. Zare, H. Yousofian-Varzaneh, Electrochim. Acta 196 (2016) 692–698.
[19] M.C. Stern, F. Simeon, T. Hammer, H. Landes, H.J. Herzog, T.A. Hatton, Energy Procedia 4 (2011) 860–867.
[20] P. Liu, B.K. Jin, F.L. Cheng, J. Electroanal. Chem. 603 (2007) 269–274.
[21] W.R. Heineman, J. Chem. Educ. 60 (1983) 305–308.
[22] C. Kvarnström, H. Neugebauer, H. Kuzmany, H. Sitter, N.S. Sariciftci, J. Electroanal. Chem. 511 (2001) 13–19.
[23] A.D. Becke, J. Chem. Phys. 98 (1993) 5648–5652.
[24] S. Hahn, H. Lee, M. Cho, J. Chem. Phys. 121 (2004) 1849–1865.
[25] B.K. Jin, L. Li, J.L. Huang, S.Y. Zhang, Y.P. Tian, J.X. Yang, Anal. Chem. 81 (2009) 4476–4481.
[26] C. Costentin, M. Robert, J.M. Saveant, Chem. Soc. Rev. 42 (2013) 2423–2436.
[27] S.W. R, K.P. Yoo, J.S. Lee, S.C. Nam, J.E. S, B.M. Min, J. Chem. Eng. Data 42 (1997) 1161–1164.